Nonlinear Dyn (2018) 93:251–258
https://doi.org/10.1007/s11071-018-4189-y

ORIGINAL PAPER

Predicting non-stationary and stochastic activation of saddle-node bifurcation in non-smooth dynamical systems

Jinki Kim · **K. W. Wang**

Received: 29 September 2017 / Accepted: 4 March 2018 / Published online: 13 March 2018

Abstract Saddle-node bifurcation can cause dynamical systems undergo large and sudden transitions in their response, which is very sensitive to stochastic and non-stationary influences that are unavoidable in practical applications. Therefore, it is essential to simultaneously consider these two factors for estimating critical system parameters that may trigger the sudden transition. Although many systems exhibit non-smooth dynamical behavior, estimating the onset of saddle-node bifurcation in them under the dual influence remains a challenge. In this work, a new theoretical framework is developed to provide an effective means for accurately predicting the probable time at which a non-smooth system undergoes saddle-node bifurcation while the governing parameters are swept in the presence of noise. The stochastic normal form of non-smooth saddle-node bifurcation is scaled to assess the influence of noise and non-stationary factors by employing a single parameter. The Fokker–Planck equation associated with the scaled normal form is then utilized to predict the distribution of the onset of bifurcations. Experimental efforts conducted using a double-well Duffing analog circuit successfully demonstrate that the theoretical framework developed in this study provides accurate prediction of the critical parameters that induce non-stationary and stochastic activation of saddle-node bifurcation in non-smooth dynamical systems.

Keywords Bifurcation · Saddle-node · Non-smooth · Piecewise-linear · Normal form · Duffing · bistable

J. Kim (✉) · K.W. Wang
Department of Mechanical Engineering, University of Michigan, Ann Arbor, MI 48109, USA
e-mail: jinkikim@umich.edu

1 Introduction

Bifurcation is an important consideration in dynamical systems since it may lead to qualitative change in the response topology by even minute variation of system parameters across the critical point [1]. In particular, saddle-node bifurcation generally induces large and sudden changes in the response amplitude since the system loses local stability as two coexisting equilibria collide and annihilate each other [1,2]. In order to exploit or avoid the dramatic changes induced by saddle-node bifurcation, it is critical to accurately estimate the onset of saddle-node bifurcation, or the conditions that induce the associated stability loss.

The classical saddle-node bifurcation in smooth dynamical systems has been extensively studied, motivated by various engineering and scientific applications including Josephson-junction circuits [3,4], micro-/nanomechanical oscillators [5,6], vibration control, energy harvesting, and sensing [7–10], chemical reactions [11], and ecological [12–14] and climate systems [15,16]. It is well known that saddle-node bifurcation is strongly affected by stochastic and non-stationary factors. For example, noise may result in premature

saddle-node bifurcations [17–19], which occur even before the governing parameter reaches the critical value that activates deterministic bifurcations. In contrast, non-stationarity of the key parameters may delay the activation of bifurcation [20,21]. It has been extensively studied to understand how the dual influence of stochastic and non-stationary factors affects the activation of smooth saddle-node bifurcations by introducing scaling laws [22–24], deriving exact and approximate responses of the stochastic normal form [25], and approximating the distribution of the escape events induced by the bifurcation [26,27].

On the other hand, non-smooth dynamics are observed in many practical systems. Examples of these systems range from mechanical devices with physical phenomena such as dry friction [28] and impact [29], robotic applications with walking and hopping mechanics [30,31], and electrical circuits with diode elements [32–35] to biological system model of neural networks [36] and economic models [37,38]. An extensive set of examples can be found in [39–41]. Although non-smooth dynamical systems have received increased attention in recent years, little is known about the bifurcations in non-smooth systems compared to those of the classical smooth systems. Since the saddle-node bifurcation induces local stability loss of the system, investigation on the bifurcation point is directly associated with stability analysis. A number of researchers have studied the stability of non-smooth dynamical systems, for example, by examining how small perturbations from the initial conditions propagate in periodic response [42,43] and evaluating the eigenvalues of the Jacobian matrix of a Poincaré map [40,44,45]. On the other hand, these advancements are focused on the steady-state response of deterministic system not considering the critical influences of noise and non-stationarity on the stability. Therefore, in this research, we investigate the coupled influence of stochastic and non-stationary factors to accurately predict the onset of non-smooth saddle-node bifurcation. While a qualitative scaling law of the time delay near non-smooth saddle-node bifurcation is introduced in [46], this study presents quantitative results about the distribution of bifurcation points, which will provide a direct means for enhancing practical applications involving non-smooth saddle-node bifurcation.

In the following sections, we first introduce a stochastic normal form of non-smooth saddle-node bifurcation that is scaled to examine the dual influence of noise and non-stationarity on the bifurcation activation by using a single parameter. Numerical and experimental investigations employing a double-well Duffing analog circuit are carried out to verify the distribution of the onset of bifurcations predicted by the theoretical framework. Following the investigations, concluding remarks summarize and reflect upon the potential of the new approach.

2 Stochastic normal form of dynamic saddle-node bifurcation

The normal form of classical saddle-node bifurcation of a smooth system

$$\dot{x} = \mu + x^2 \tag{1}$$

exhibits two equilibria for bifurcation parameter $\mu < 0$, where fixed point $x^* = -\sqrt{\mu}$ is stable while $x^* = \sqrt{\mu}$ is unstable. When the parameter $\mu < 0$ quasi-statically increases, the system becomes unstable as saddle-node bifurcation occurs at $\mu = 0$ annihilating the two equilibria (Fig. 1a), and the response of the system escapes from the dynamics local to the bifurcation point and generally jumps to other stable equilibrium of the system.

Non-smooth continuous systems can generally be put in the formulation of Filippov systems [39], and Eq. (2) is one of the simple formulations that represent the dynamical characteristics of saddle-node bifurcations in non-smooth continuous systems.

$$\dot{x} = \mu + |x|\,, \tag{2}$$

This system has two equilibria $x = \pm\mu$ for $\mu < 0$ as shown in the bifurcation diagram of Fig. 1b. Since Eq. (2) not only exhibits topologically similar bifurcation diagram to the one for saddle-node bifurcation in continuous systems but also can be approximated as limits of smooth bifurcations [40], it is considered as the non-smooth counterpart of saddle-node bifurcation in this study. Various saddle-node bifurcations in non-smooth continuous systems (for example, stick–slip oscillations [47] and electrical circuits with diodes [33]) can be represented by Eq. (2) via proper scaling and coordinate changes.

To investigate the stochastic and non-stationary influences on the activation of saddle-node bifurca-

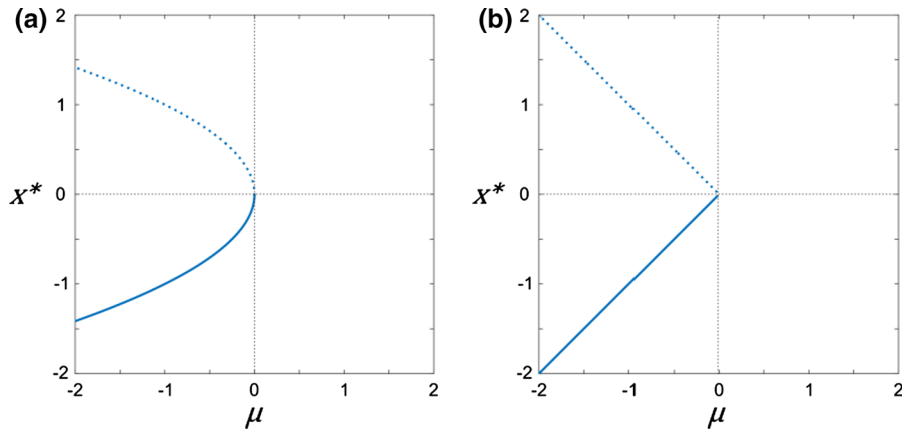

Fig. 1 Bifurcation diagrams of **a** smooth and **b** non-smooth saddle-node bifurcation. Solid (dotted) lines indicate (un)stable fixed points

tions, we utilize the stochastic normal form of the saddle-node bifurcation

$$\dot{x} = \mu(t) + |x| + D\xi, \tag{3}$$

where D is effective noise strength and ξ is Gaussian white noise with autocorrelation $\langle \xi(t)\,\xi(\tilde{t})\rangle = 2\delta(t-\tilde{t})$. The non-stationary influence on the saddle-node bifurcation is assessed by examining the system stability with respect to a time-dependent bifurcation parameter $\mu(t)$. For a common case of broad practical applications, a first-order Taylor expansion of $\mu(t)$ in time is employed in this analysis, such that

$$\mu(t) = \mu_0 + rt. \tag{4}$$

In this research, we assume that the bifurcation parameter is swept from $\mu_0 < 0$ at a sweep rate of $r > 0$. Since the bifurcation parameter $\mu(t)$ varies linearly in time, new time and spatial coordinates can be defined by incorporating the parameter sweep rate as follows,

$$\tau = \mu r^{-1}, \tag{5}$$

$$z = x r^{-1}. \tag{6}$$

Note that the bifurcation occurs at $\tau = 0$ for ideal condition without noise and non-stationarity where the bifurcation point is $\mu = 0$. By substituting Eqs. (5, 6) into (3), we can obtain a new normal form

$$z' = \tau + |z| + \alpha\xi, \tag{7}$$

$$\alpha = D/r, \tag{8}$$

where $(\,)'$ indicates differentiation with respect to new time variable τ. As a result, one can utilize a single parameter, scaled noise level α, to investigate the dual influence of noise and non-stationarity on the activation of non-smooth saddle-node bifurcation.

Since the normal form describes the local dynamics near bifurcation point, when bifurcation is activated the system trajectories become very steep diverging to infinity. Therefore, in order to investigate the distribution of bifurcation events, our goal is to determine the distribution of escape time T at which the response of Eq. (7) becomes unbounded, i.e., $z(T) \to \infty$. The Fokker–Planck equation (FPE) [48] can be derived from the scaled stochastic normal form (Eq. 7) as

$$\frac{\partial \rho(z,\tau)}{\partial \tau} = -\frac{\partial}{\partial z}\left[(\tau + |z|)\,\rho(z,\tau)\right] + \alpha^2 \frac{\partial^2 \rho(z,\tau)}{\partial z^2}, \tag{9}$$

where $\rho(z,\tau)$ is the probability density function (PDF) for finding the system at z at time τ. By solving the FPE, the diffusive characteristics of the newly derived Langevin equation (Eq. 7) can be obtained, which follows the scaling law of Brownian motion where the standard deviation of probability distribution increases proportionally to square root of time τ.

In this work, we assume that the escape time T at which the system reaches a large value ($z_\infty \gg 1$) is equivalent to the time taken to infinity. The probability $P_\infty(T)$ that the system has escaped to infinity by time $\tau = T$ can be determined by subtracting the probability that the system exists in a finite domain at time T from unity as

$$P_\infty(T) = 1 - \int_{-\infty}^{z_\infty} \rho(z,T)\,\mathrm{d}z, \tag{10}$$

which is a cumulative distribution function of escape events. The PDF $P(T)$ for bifurcations activated at time T can be obtained as

$$P(T) = \frac{d}{dT} P_{\infty}(T). \tag{11}$$

Solving the Fokker–Planck equation becomes extremely computationally heavy for large noise levels since larger spatial domain is required for integration as the probability distribution of the bifurcation points spatially spreads out. For conditions with $\alpha \gg 1$ where bifurcation parameter μ increases relatively slowly with respect to the noise level D, or the noise level is much greater than the sweep rate, one can assume that the bifurcation parameter is adiabatically swept through the critical value and the system exhibits noise-induced escapes. As a result, the rate of escape events can be approximated by the well-known Kramers' rate $W(\tau)$ (Eq. 12) and the approximate PDF $P_K(T)$ of escape at time T can be determined by Eq. (13) [17]

$$W(\tau) = \frac{1}{2\pi} \exp\left(-\frac{(-\tau)^2}{\alpha^2}\right), \tag{12}$$

$$P_K(T) = W(T) \exp\left(-\int_{\tau_0}^{T} W(\tau)\, d\tau\right), \tag{13}$$

where the initial condition is assumed to be $\tau_0 = -\infty$.

In summary, the key result is that the stochastic and non-stationary activation of non-smooth saddle-node bifurcation can be estimated by using a single parameter, scaled noise α in Eq. (8). The PDF of bifurcation points is estimated as Eq. (11) by solving the Fokker–Planck equation, which can be approximated as Eq. (13) in the slow sweeping (or large noise) limit ($\alpha \gg 1$). The distribution of escape time T can be used to assess the bifurcation point, or the actual critical parameter value, that triggers the bifurcation by straightforward back-calculation from Eq. (5).

3 Numerical and experimental investigation

In this section, the theoretical prediction of the escape statistics utilizing the scaled normal form of non-smooth saddle-node bifurcation is validated through numerical and experimental investigations. Figure 2a shows a schematic diagram of a double-well Duffing analog circuit employed in this research. This circuit exhibits bistability with piecewise-linear characteristics introduced by nonlinear feedback loop among an op-amp and a pair of antiparallel diodes, i.e., diodes with two terminals shortened in opposite directions. As a result, non-smooth saddle-node bifurcation occurs when the excitation amplitude of the circuit increases while the excitation frequency is fixed below the linear resonance frequency. By virtue of the saddle-node bifurcation that activates drastic transitions between the intra- and interwell oscillations in

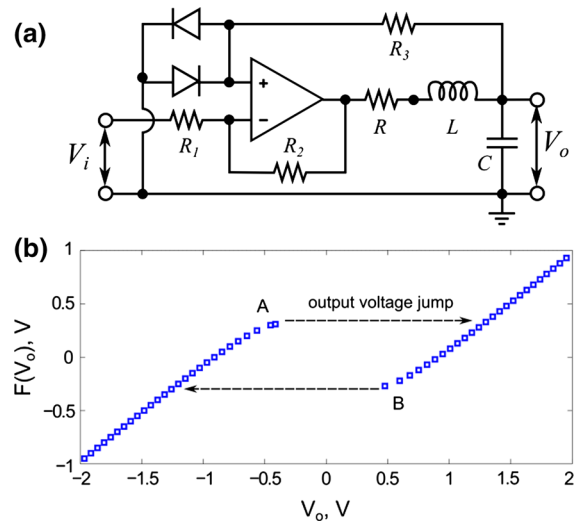

Fig. 2 **a** Schematic diagram of the double-well Duffing analog circuit utilized in experimental analysis. **b** Experimentally measured nonlinear voltage function of the circuit with respect to output voltage amplitude

the output voltage level, the bistable circuit has been successfully utilized for several applications including bifurcation-based sensing for detecting parameter changes and damages in structures [34,35].

The governing equation of the bistable circuit can be derived by assuming ideal op-amp and diode characteristics as follows [34,49].

$$LC\ddot{V}_o + RC\dot{V}_o + F(V_o) = V_i, \tag{14}$$

$$F(V_o) = \begin{cases} V_o - gV_D, & V_o > V_D \\ (1-g)V_o, & |V_o| \le V_D \\ V_o + gV_D, & V_o < -V_D \end{cases}, \tag{15}$$

where L, C, R, and $F(V_o)$ represent the inductance, capacitance, resistance, and a nonlinear voltage function, respectively; V_i, V_o, and V_D, respectively, indicate the input and output voltage amplitudes of the bistable circuit, and voltage drop over an open diode; and the overdot indicates a time derivative. Following ideal op-amp assumption, the feedback gain is $g = 1 + R_2/R_1$. The op-amp employed in this research is LM741CN, and the diodes are 1N4148. The other relevant circuit parameters are provided in Table 1.

Considering the overdamped limit of large damping, the term $LC\ddot{V}_0$ can be neglected. Although the circuit exhibits two saddle-node bifurcations as the amplitude of harmonic excitation is increased and decreased, for consistency we focus on the saddle-node bifurcation that occurs for increasing amplitude of the excitation. When small perturbations $\eta = V_i - V_i^{cr}$ and $x = V_o - V_o^{cr}$ near a critical fixed point $\left(V_i^{cr}, V_o^{cr}\right) = ((g-1)V_D, -V_D)$ at

Table 1 Experimental system parameters of the double-well Duffing analog circuit

L (mH)	C (uF)	R (Ω)	R_1 (kΩ)	R_2 (kΩ)	R_3 (kΩ)
10.24	0.96	800	9.07	9.08	10

Table 2 Scaled noise level α for each sweep rate and additive noise level applied in the experimental investigation

Sweep rate (mV/s)	0.5	2	10	10	10	10
Noise level (mV rms)	10	50	10	50	100	100
α	9.2	7.4	184.1	36.8	18.4	7.4
Sweep rate (mV/s)	50	50	50	50	50	50
Noise level (mV rms)	10	50	100	250	500	1000
α	920.7	184.1	92.1	36.8	18.4	9.2

which the bifurcation is induced for deterministic system are introduced and substituted into Eqs. (14, 15), the local dynamics around the bifurcation point can be expressed by

$$\dot{x} = \frac{1}{\mathrm{RC}} \left(\eta + |x|\right). \tag{16}$$

By assuming the stochastic influence as an additive Gaussian white noise term $D\xi$ [50] and scaling the variables as $\tau = \mu \left(r_V \mathrm{RC}\right)^{-1}$ and $z = x \left(r_V \mathrm{RC}\right)^{-1}$ in a similar manner to Eqs. (5, 6), we finally derive a scaled normal form of non-smooth saddle-node bifurcation:

$$z' = \tau + |z| + \alpha_V \xi. \tag{17}$$

r_V is input voltage amplitude sweep rate and scaled noise level $\alpha_V = \frac{D}{\mathrm{RC} r_V}$.

Figure 2b displays the qualitative piecewise-linear characteristics of the nonlinear voltage function $F\left(V_\mathrm{o}\right)$ of the bistable circuit, which corresponds to the smooth restoring force of a conventional double-well Duffing oscillator expressed by a cubic polynomial with negative linear and positive cubic terms [51,52]. The voltage function is experimentally obtained by measuring the output voltage V_o while quasi-statically varying the DC input voltage within the range that encompasses the two stable equilibria of the bistable circuit. Starting from large negative value, when the DC input voltage is quasi-statically increased around 0.32 V, indicated as point A in Fig. 2b, bifurcation is activated and the output voltage V_o undergoes a sudden transition from approximately -0.42 V to 1.30 V. For decreasing input voltage level, the bistable circuit exhibits a symmetric behavior of jump event due to the bifurcation. The critical fixed point $\left(V_i^\mathrm{cr}, V_\mathrm{o}^\mathrm{cr}\right)$ in this analysis can be determined as $(0.32, -0.42)$. On the other hand, due to the practical factors ignored in the ideal diode model, such as temperature effect and nonlinearity in the diode [53], the slope near the bifurcation point decreases as shown in Fig. 2b. To account for these effects, the slope was measured ($a \approx 0.2$) and considered in the normal form derivation, yielding $\alpha_V = \frac{aD}{\mathrm{RC} r_V}$.

The double-well Duffing analog circuit is harmonically excited at 35 Hz, and the input voltage amplitude is increased by sweeping across the bifurcation point starting from 0.3 to 0.4 V. In addition to the ambient noise level, different levels of Gaussian white noise are added to the excitation input voltage to examine the stochastic influences on the saddle-node bifurcation activation. The root-mean-square (rms) amplitude of the ambient noise in the experiment is 0.015 mV. The input voltage amplitude sweep rates and the additive noise levels applied in the experiment are given in Table 2. Note that the sweep conditions and noise levels are in the range that does not induce other bifurcation in the bistable circuit, which satisfies the assumption of utilizing the normal form for analysis in this work. The input voltage amplitude V_esc that triggers non-smooth saddle-node bifurcation is recorded and utilized to derive the scaled escape time $T = \left(V_\mathrm{esc} - V_i^\mathrm{cr}\right) / \left(\mathrm{RC}\, r_V\right)$. Note that the scaled escape time is greater than zero when delayed bifurcation occurs, while it gives negative value for premature bifurcations. The mean and standard deviation of the escape time are obtained from 100 runs for each condition with various sweep rates and noise levels.

Figure 3 shows 20 sample paths (solid curves) obtained by solving Eq. (17) using the Euler–Maruyama method [54] for three different noise levels ($\alpha = 2, 10, 50$). These trajectories are compared with the mean and two standard deviations obtained by solving the Fokker–Planck equa-

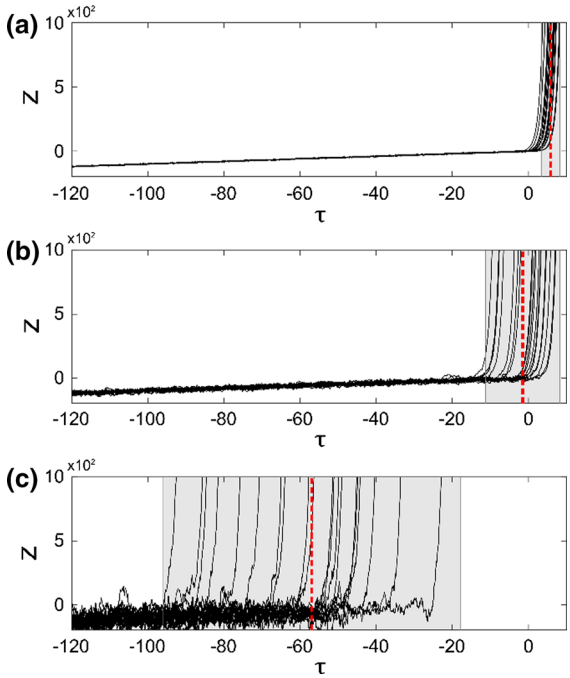

Fig. 3 Comparison of 20 sample paths of Eq. (7) with the predicted mean (dashed line) and two standard deviations (shaded area) of escape time for three scaled noise level: **a** $\alpha = 2$, **b** $\alpha = 10$, **c** $\alpha = 50$

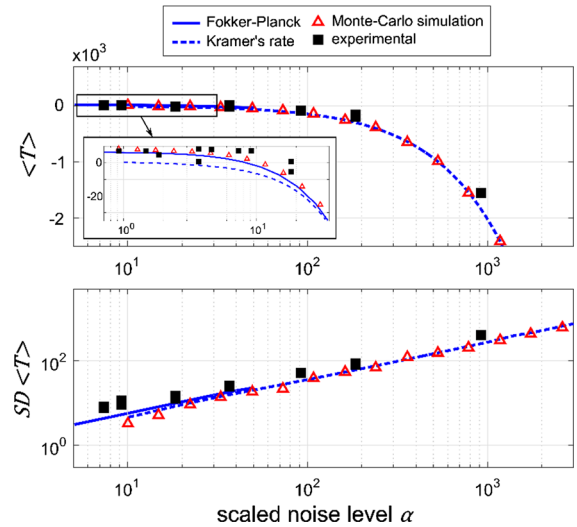

Fig. 4 The analytically predicted mean and standard deviation of escape time T using Fokker–Planck equation (solid line) and Kramer's rate (dashed line) are compared with the results obtained by Monte–Carlo simulation (triangle), and experimental measurement (square) with respect to the scaled noise level α. Inset figure shows zoomed view for small α

tion, which are plotted as vertical dashed lines and shaded areas, respectively. The initial condition is selected to be $\tau_0 = -120$, while theoretically assumed as $\tau_0 = -\infty$, and the spatial domain of $z = [-1000, 1000]$ is selected for solving the FPE. It is assumed that the system has escaped to infinity when $z > 1000$. Figure 3 shows that the displacements indicated along the vertical axis increase to infinity as bifurcations are activated, and the bifurcations occur earlier for larger noise level. It can be clearly observed that the statistical characteristics of bifurcation points are accurately estimated for different noise levels α. Since α is a scaled noise level that incorporates both noise and non-stationarity influences (Eq. 8), one can reliably predict the statistical characteristics of bifurcation points influenced by the combination of these dual factors.

In Fig. 4, the mean and standard deviation of the escape times estimated by the theoretical framework using Fokker–Planck equation (solid curve) are plotted with the experimentally obtained results (square) with respect to a broad range of scaled noise level α. Since solving the FPE becomes computationally expensive for large noise levels, the theoretical bifurcation distributions are estimated by the Kramers' rate approximation (dashed line) for large- scaled noise level. In addition, Monte–Carlo-based results (triangle) obtained by numerically solving the scaled stochastic normal form in Eq. (17) for 1000 times via Euler–Maruyama method [54] are included in Fig. 4 for comparison. It can be observed that the escape statistics estimated by the scaled normal form are in good agreement with the numerically and experimentally determined results for a wide range of scaled noise level.

Both of the delayed and premature escape events in the bistable circuit are successfully predicted for small and large values of scaled noise level, respectively. For weak noise level or relatively fast sweep rate, the bifurcation is delayed ($T > 0$) compared to quasi-statically activated bifurcation point ($T = 0$). On the other hand, for large-scaled noise level, the mean of escape time T decreases below zero, while the standard deviation increases. In other words, bifurcations may occur even for conditions where the bifurcation parameter is much smaller than the bifurcation point for ideal condition without noise and non-stationarity. Although the initial condition is theoretically assumed to be $\tau_0 = -\infty$, in real-world implementations if the initial condition is selected not sufficiently far from the bifurcation point, escape events may be immediately activated as can be observed in Fig. 3c where $\tau_0 = -120$. Therefore, it is critical to accurately estimate the bifurcation distribution so that one can exploit or steer the activation of bifurcations. Overall, the experimental and numerical investigation results obtained for a wide range of bifurcation parameter sweep rates and noise levels strongly support and validate the prediction

obtained by the proposed scaled normal form Eq. (7). The theoretical analysis derived based on the new scaled normal form herein will provide an effective means for predicting the onset of critical transitions related to saddle-node bifurcation in a variety of non-smooth systems under non-stationary and stochastic influences.

4 Conclusion

The non-stationary and stochastic influences on the activation of non-smooth saddle-node bifurcation are investigated to develop an analytical strategy for predicting critical parameters that activate escape from a stable equilibrium. A new scaled normal form of non-smooth saddle-node bifurcation is developed, which enables exploring the dual influence on the escape event by using a single parameter. The distribution of the onset of bifurcation is then quantitatively predicted from the Fokker–Planck equation corresponding to the scaled normal form. Numerical and experimental investigations using a double-well Duffing analog circuit successfully verify the accuracy of the predictions obtained by the theoretical framework. Since the predictive strategy developed here is based on normal form analysis, it is expected that this new method will provide a straightforward and accurate means for estimating critical conditions that lead to sudden large jumps in the response of various practical contexts associated with non-smooth saddle-node bifurcation.

Acknowledgements This research was partially supported by the National Science Foundation under Award Nos. 1232436 and 1661568 and the University of Michigan Collegiate Professorship fund.

References

1. Kuznetsov, Y.: Elements of Applied Bifurcation Theory, 2nd edn. Springer, New York (1998)
2. Kovacic, I., Brennan, M.: The Duffing Equation: Nonlinear Oscillators and Their Behaviour. Wiley, Hoboken (2011)
3. Devoret, M., Esteve, D., Martinis, J., Cleland, A., Clarke, J.: Resonant activation of a Brownian particle out of a potential well: microwave-enhanced escape from the zero-voltage state of a Josephson junction. Phys. Rev. B **36**(1), 58–73 (1987)
4. Vijay, R., Devoret, M., Siddiqi, I.: Invited review article: the Josephson bifurcation amplifier. Rev. Sci. Instrum. **80**(11), 111101 (2009)
5. Aldridge, J., Cleland, A.: Noise-enabled precision measurements of a Duffing nanomechanical resonator. Phys. Rev. Lett. **94**(15), 156403 (2005)
6. Stambaugh, C., Chan, H.: Noise-activated switching in a driven nonlinear micromechanical oscillator. Phys. Rev. B **73**(17), 172302 (2006)
7. Harne, R.L., Wang, K.W.: Harnessing Bistable Structural Dynamics: For Vibration Control, Energy Harvesting and Sensing. Wiley, Hoboken (2017)
8. Johnson, D.R., Thota, M., Semperlotti, F., Wang, K.W.: On achieving high and adaptable damping via a bistable oscillator. Smart Mater. Struct. **22**(11), 115027 (2013)
9. Wu, Z., Harne, R.L., Wang, K.W.: Energy harvester synthesis via coupled linear-bistable system with multi-stable dynamics. ASME J. Appl. Mech. **81**(6), 061005 (2014)
10. Harne, R.L., Wang, K.W.: A bifurcation-based coupled linear-bistable system for microscale mass sensing. J. Sound Vib. **333**(8), 2241–2252 (2014)
11. Koper, M.: Non-linear phenomena in electrochemical systems. J. Chem. Soc. Faraday Trans. **94**(10), 1369–1378 (1998)
12. Dakos, V., van Nes, E., D'Odorico, P., Scheffer, M.: Robustness of variance and autocorrelation as indicators of critical slowing down. Ecology **93**(2), 264–271 (2012)
13. Scheffer, M., Carpenter, S., Lenton, T., Bascompte, J., Brock, W., Dakos, V., van de Koppel, J., van de Leemput, I., Levin, S., van Nes, E., Pascual, M., Vandermeer, J.: Anticipating critical transitions. Science **338**(6105), 344–348 (2012)
14. D'Souza, K., Epureanu, B., Pascual, M.: Forecasting bifurcations from large perturbation recoveries in feedback ecosystems. PLoS ONE **10**(9), e0137779 (2015)
15. Lenton, T.: Early warning of climate tipping points. Nat. Clim. Change **1**(4), 201–209 (2011)
16. Scheffer, M., Bascompte, J., Brock, W., Brovkin, V., Carpenter, S., Dakos, V., Held, H., van Nes, E., Rietkerk, M., Sugihara, G.: Early-warning signals for critical transitions. Nature **461**(7260), 53–59 (2009)
17. Hanggi, P.: Escape from a metastable state. J. Stat. Phys. **42**(1–2), 105–148 (1986)
18. Meunier, C., Verga, A.: Noise and bifurcations. J. Stat. Phys. **50**(1–2), 345–375 (1988)
19. Dykman, M., Schwartz, I., Shapiro, M.: Scaling in activated escape of underdamped systems. Phys. Rev. E **72**(2), 021102 (2005)
20. Lu, C.-H., Evan-Iwanowski, R.: The nonstationary effects on a softening Duffing oscillator. Mech. Res. Commun. **21**(6), 555–564 (1994)
21. Mandel, P., Erneux, T.: The slow passage through a steady bifurcation: delay and memory effects. J. Stat. Phys. **48**(5–6), 1059–1070 (1987)
22. Breban, R., Nusse, H., Ott, E.: Scaling properties of saddle-node bifurcations on fractal basin boundaries. Phys. Rev. E **68**(6), 066213 (2003)
23. Berglund, N., Gentz, B.: Noise-Induced Phenomena in Slow-Fast Dynamical Systems: A Sample-Paths Approach. Springer, New York (2006)
24. Kuehn, C.: Multiple Time Scale Dynamics. Springer, New York (2015)
25. Nicolis, C., Nicolis, G.: Dynamical responses to time-dependent control parameters in the presence of noise: a normal form approach. Phys. Rev. E **89**(2), 022903 (2014)
26. Miller, N., Shaw, S.: Escape statistics for parameter sweeps through bifurcations. Phys. Rev. E **85**(4), 046202 (2012)
27. Kim, J., Harne, R.L., Wang, K.W.: Predicting non-stationary and stochastic activation of saddle-node bifurcation. J. Comput. Nonlinear Dyn. **12**(1), 011009 (2016)

28. Leine, R., Van Campen, D., Keultjes, W.: Stick-slip whirl interaction in drillstring dynamics. J. Vib. Acoust. **124**(2), 209–220 (2002)
29. Sung, C., Yu, W.: Dynamics of a harmonically excited impact damper: bifurcations and chaotic motion. J. Sound Vib. **158**(2), 317–329 (1992)
30. Holmes, P., Full, R., Koditschek, D., Guckenheimer, J.: The dynamics of legged locomotion: models, analyses, and challenges. SIAM Rev. **48**(2), 207–304 (2006)
31. Iqbal, S., Zang, X., Zhu, Y., Zhao, J.: Bifurcations and chaos in passive dynamic walking: a review. Robot. Auton. Syst. **62**(6), 889–909 (2014)
32. Chua, L.: Chua's circuit 10 years later. Int. J. Circuit Theory Appl. **22**(4), 279–305 (1994)
33. di Bernardo, M., Budd, C., Champneys, A., Kowalczyk, P., Nordmark, A., Tost, G., Piiroinen, P.: Bifurcations in nonsmooth dynamical systems. SIAM Rev. **50**(4), 629–701 (2008)
34. Harne, R.L., Wang, K.W.: Robust sensing methodology for detecting change with bistable circuitry dynamics tailoring. Appl. Phys. Lett. **102**(20), 203506 (2013)
35. Kim, J., Harne, R.L., Wang, K.W.: Enhancing structural damage identification robustness to noise and damping with integrated bistable and adaptive piezoelectric circuitry. J. Vib. Acoust. **137**(1), 011003 (2015)
36. Zhao, X., Schaeffer, D., Berger, C., Krassowska, W., Gauthier, D.: Cardiac alternans arising from an unfolded border-collision bifurcation. J. Comput. Nonlinear Dyn. **3**(4), 041004 (2008)
37. Caballé, J., Jarque, X., Michetti, E.: Chaotic dynamics in credit constrained emerging economies. J. Econ. Dyn. Control **30**(8), 1261–1275 (2006)
38. Mosekilde, E., Laugesen, J.: Nonlinear dynamic phenomena in the Beer model. Syst. Dyn. Rev. **23**(2–3), 229–252 (2007)
39. Simpson, D.: Bifurcations in Piecewise-Smooth Continuous Systems. World Scientific, Singapore (2010)
40. Leine, R., Nijmeijer, H.: Dynamics and Bifurcations of Non-Smooth Mechanical Systems. Springer, New York (2013)
41. di Bernardo, M., Budd, C., Champneys, A., Kowalczyk, P.: Piecewise-Smooth Dynamical Systems: Theory and Applications. Springer, New York (2008)
42. Masri, S., Caughey, T.: On the stability of the impact damper. J. Appl. Mech. **33**(3), 586–592 (1966)
43. Natsiavas, S.: Periodic response and stability of oscillators with symmetric trilinear restoring force. J. Sound Vib. **134**(2), 315–331 (1989)
44. Shaw, S., Holmes, P.: A periodically forced piecewise linear oscillator. J. Sound Vib. **90**(1), 129–155 (1983)
45. Luo, A.: The mapping dynamics of periodic motions for a three-piecewise linear system under a periodic excitation. J. Sound Vib. **283**(3), 723–748 (2005)
46. Kuehn, C.: Scaling of saddle-node bifurcations: degeneracies and rapid quantitative changes. J. Phys. A Math. Theor. **42**(4), 045101 (2008)
47. Dankowicz, H., Nordmark, A.B.: On the origin and bifurcations of stick-slip oscillations. Phys. D **136**(3), 280–302 (2000)
48. Risken, H.: The Fokker–Planck Equation. Springer, Berlin (1989)
49. Tamaševičius, A., Mykolaitis, G., Pyragas, V., Pyragas, K.: Delayed feedback control of periodic orbits without torsion in nonautonomous chaotic systems: theory and experiment. Phys. Rev. E **76**(2), 026203 (2007)
50. Forgoston, E., Schwartz, I.: Escape rates in a stochastic environment with multiple scales. SIAM J. Appl. Dyn. Syst. **8**(3), 1190–1217 (2009)
51. Holmes, P.: A nonlinear oscillator with a strange attractor. Philos. Trans. R. Soc. Lond. A Math. Phys. Eng. Sci. **292**(1394), 419–448 (1979)
52. Kovacic, I., Brennan, M.J.: The Duffing Equation: Nonlinear Oscillators and Their Behaviour. Wiley, Hoboken (2011)
53. Rizzoni, G.: Fundamentals of Electrical Engineering. McGraw-Hill, New York (2009)
54. Higham, D.: An algorithmic introduction to numerical simulation of stochastic differential equations. SIAM Rev. **43**(3), 525–546 (2001)